COMPACT FRACTURE MECHANICS-BASED SENSOR FOR MONITORING ENVIRONMENT ASSISTED CRACKING

N. K. Brown and F. J. Friedersdorf
Luna Innovations Incorporated
706 Forest Street, Suite A
Charlottesville, VA 22903

ABSTRACT

Environment assisted cracking (EAC) has long been recognized as a major cause of component and structural failures, but the basic mechanisms of this process are still not fully understood. The development of practical methods of testing and monitoring these degradation mechanisms is critical to understanding the kinetics of such failures and also to providing maintainers with an indication of operating conditions that have the potential to produce EAC in their systems.

To meet this need, Luna has developed a compact EAC sensing device to provide valuable early warning capability, alerting users to environmental conditions perquisite to cracking within their structures. The primary sensing element employs a circumferentially notched tensile sample of similar material as the monitored structure. The sample is preloaded to emulate the nominal stresses in the structure. Electrically coupling the sample to the structure places it under similar electrochemical conditions. Crack propagation is monitored by observing preload shedding with an embedded load cell. An onboard Ag/AgCl reference electrode provides a secondary indicator of cracking potential. Luna has achieved crack depth resolution of better than a micron over a range of several millimeters, permitting observation of crack velocities on the order of 0.1 nanometer/sec (0.0001 μm/sec) within hours. With this system, crack velocity dependence on potential for 17-4 PH SS and Monel K500™ alloys were characterized, and non-zero crack velocities were observed within typical sacrificial anode potential ranges in seawater.

Keywords: cracking, hydrogen embrittlement, structural health monitoring, cathodic protection

INTRODUCTION

Environment assisted cracking (EAC) includes hydrogen embrittlement (HE) and stress corrosion cracking (SCC) and other forms of metal and alloy cracking caused by the combined action of stress and environment. In general, hydrogen embrittlement (HE) is the process by which various metals, such as high-strength alloys, lose ductility and crack due to hydrogen exposure. The process is associated with hydrogen uptake in the alloy that may occur due to galvanic coupling or polarization by cathodic protection systems. The combination of atomic hydrogen, alloy properties, and applied stress can result in embrittlement and crack propagation.

In marine environments, fasteners and other high-strength components may become hydrogen embrittled under non-ideal cathodic protection conditions. Embrittled material, in conjunction with high tensile loads and local stress risers that are characteristic of typical bolting applications (e.g., threads, surface imperfections), can result in environment assisted cracking and subsequent fastener failure that has significant safety and availability implications for a variety of marine applications. An *in situ* EAC sensing device would provide valuable early warning capability, alerting operators to environmental conditions that are prerequisite to cracking within the monitored structure. In addition to monitoring existing structures, such a compact device would be useful during the development and qualification of new alloys by permitting crack propagation studies in relevant environments (e.g., shipboard). This paper presents Luna's recent work to develop a small, deployable EAC monitoring system and representative crack propagation test results in 17-4 PH stainless steel and Monel K500 sample materials.

SENSOR DESIGN

To monitor for conditions that are likely to produce EAC in the monitored structure, the sensing platform utilizes two distinct sensing strategies. The primary element features a surrogate fracture specimen loaded to produce similar stress intensities as expected in the monitored structure such that cracking will initiate and propagate when a critical amount of hydrogen ingress has occurred. The sensor infers sample crack depth by monitoring the sample's tensile load that sheds predictably as the crack propagates. As a secondary indicator of environmental severity, the sensor provides an electrochemical potential measurement using a Ag/AgCl reference electrode as commonly employed for marine cathodic protection systems. These two elements are combined in a single housing along with the electronics for signal conditioning, data storage, and communications and battery power (Figure 1). The remainder of this section will discuss the design considerations of the fracture mechanics transducer.

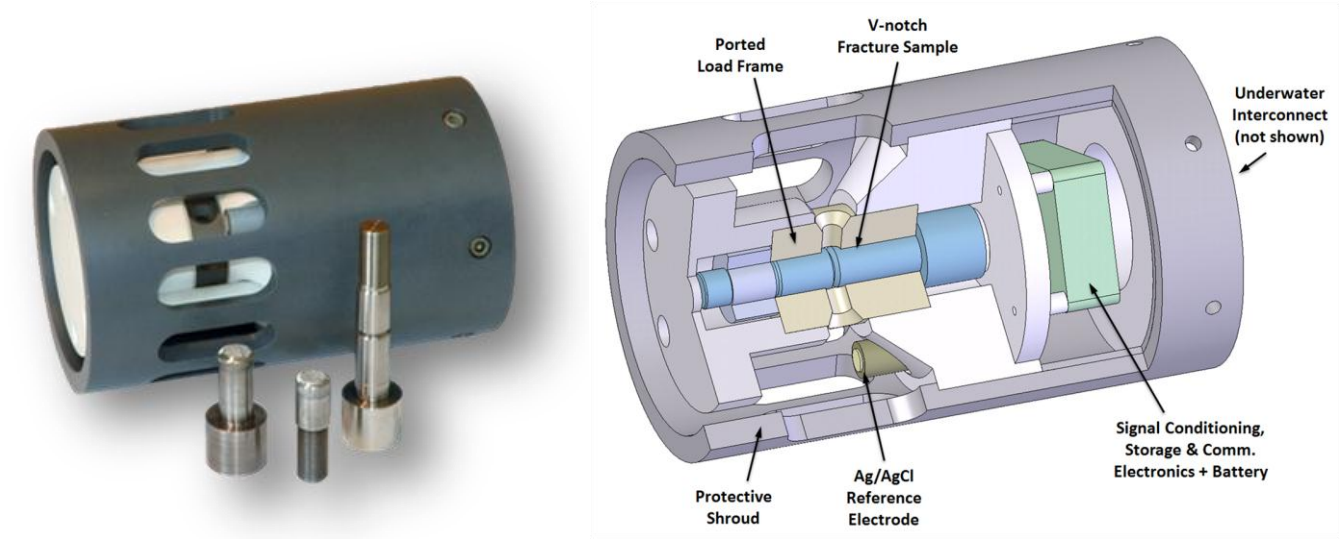

Figure 1. EAC sensor node assembly (left), and cutaway view (right). Sensor diameter is 114 mm [4.5 in].

Crack Sensor Overview

To provide real-time indication of crack growth in a surrogate sample, the crack sensor design consists of four major components: tensile sample, ported frame, compression load cell, and preload nut (Figure 2). Advancing the pre-load nut places the sample in tension and the frame/load cell into equal and opposite compression, the force of which is measured with the compression load cell. The

sample and frame are designed intentionally very stiff to approximate a constant-strain configuration, such that increasing sample compliance due to crack growth in the notch will produce a measurable drop in tensile load. Nominally, the selected frame and sample materials will have similar thermal expansion characteristics so that changes in environmental temperature do not affect the effective strain (i.e. measured force).

During the preload operation, a hydraulic load fixture is used to load the tensile sample and reduce the tightening torque needed to achieve the desired pre-strain, minimizing the torsional load imparted to the specimen. Tight clearances and flatness/perpendicularity tolerances in the sensor construction ensure uniaxial load, minimal misalignment, easy assembly, and enhances assembly stiffness. With the sample electrically connected to the monitored structure, the ported frame permits seawater and potential field line ingress to the sample notch region. A cast epoxy layer electrically isolates the metal frame from the surrounding fluid such that only the notched portion of the tensile sample is directly in contact with the seawater. This feature minimizes the surface area to be driven by the cathodic protection system and prevents undue embrittlement of the frame component.

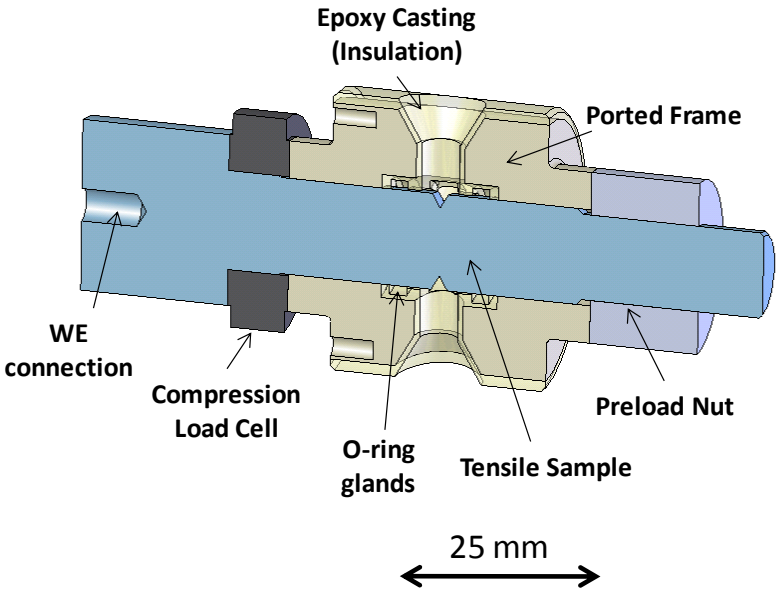

Figure 2. Primary EAC sensor components.

Tensile Sample Design

Sample geometry is an important consideration for the direct crack measurement device. The primary concerns include: measurement sensitivity, overall size, ease of fabrication, and cost. Luna selected a circumferentially notched tensile (CNT) specimen geometry, as it is the smallest possible geometry that can produce valid plane-strain crack loading conditions, within 3% of standard ASTM compact tension (CT) specimens[1]. To produce valid plane-strain conditions, the plastic zone ahead of the crack tip must be small relative to the surrounding geometry. The CNT specimen can be made smaller thanks to its continuous circumferential notch that affords a highly constrained plastic zone. CT specimens, on the other hand, must be much wider to ensure that the plane stress conditions at the free edges are small compared to the plane strain in the central region.

In addition to the size advantage, cost is a significant driver for the CNT geometry. Compared with standard CT specimens, the preparation cost for the cylindrical CNT specimen can be significantly less, up to an order of magnitude[2]. The greatly simplified loading frame geometry permitted by the CNT specimen further reduces the overall sensor cost. Finally, the CNT geometry can be designed such that its compliance is highly sensitive to crack growth in the notch, with a typical engineering tradeoff between sensitivity and overall range. The key to maintaining crack depth sensitivity is keeping the sample as short as practical to maximize initial stiffness, as discussed in the following section.

Crack Depth Measurement

Converting the sensor's raw force output to a more useful crack depth indication required development of calibration curves relating the sensor assembly's compliance to sample crack depth, as described below.

As described by Equation 1, the effective force imparted to the sample (F) is simply the product of the sensor assembly stiffness (k) and the total deflection of all the components (x), where the latter is equivalent to the preload nut advance distance. Once the initial preload is set, the nut position, and thus x, is constant over the life of the sensor. Therefore, the measured force is a direct indicator of the assembly stiffness and can be used to estimate crack depth if the relationship between assembly stiffness and crack depth is known.

The mechanics of the sensor assembly may be best envisioned as two springs in series (Figure 3), where $k_s(a)$ is the sample stiffness at crack depth a, $F(a)$ is the measured force at crack depth a, and x is the total deflection of both frame and sample. All of the non-sample component stiffnesses are assumed to be constant and may be lumped into a single 'frame' stiffness, k_f. The overall assembly stiffness, $k(a)$, is the series combination of the two stiffness components:

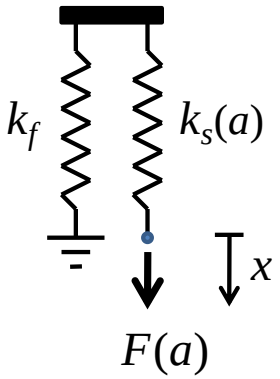

Figure 3. Mechanical representation of the sensor assembly.

$$F(a) = k(a)\,x \qquad \text{(Equation 1)}$$

$$k(a) = \frac{k_f\,k_s(a)}{k_f + k_s(a)} \qquad \text{(Equation 2)}$$

The sample stiffness vs. crack depth, $k_s(a)$ may be accurately characterized through numerical finite element analysis (FEA) modeling of the sample geometry (Figure 4). The crack plane is constrained axially to simulate a connection between the two sample halves, and permits a convenient method of 'unzipping' the crack to simulate concentric, radial crack propagation. Stiffness at each crack depth is determined by applying a known tensile load to the sample and observing the deflection between the load bearing faces on the bolt head and nut.

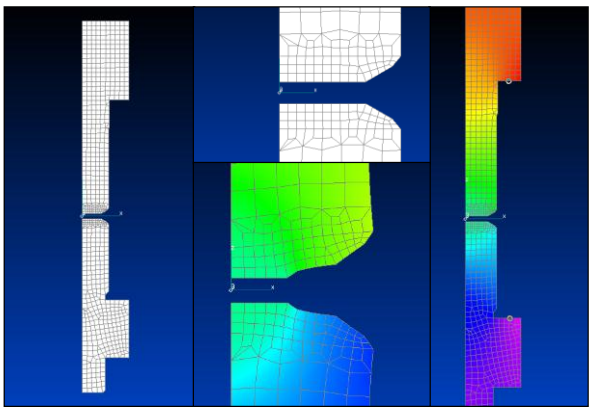

Figure 4. FEA model of fracture sample (left), crack plane detail (middle) and deflection measurement between load bearing surfaces (right).

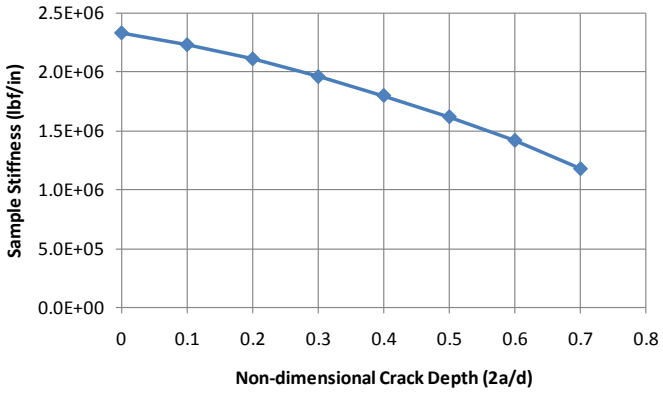

Figure 5. FEA results for sample stiffness vs. crack depth (Monel K-500, d = 10.16 mm).

Figure 6. Empirical determination of assembly stiffness by measuring length at several preloads.

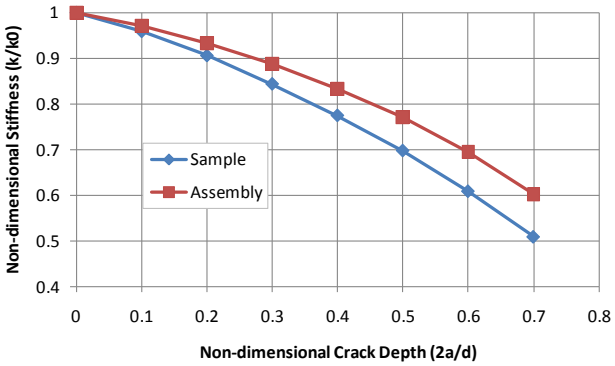

Figure 7. Normalized stiffness vs. crack depth for the sample alone and the combined assembly.

The numerical results illustrating sample stiffness vs. crack depth are presented as the blue trace in Figure 7 for K-500 alloy, assuming an elastic modulus of E = 176 GPa and Poisson's ratio of ν = 0.3. Radial crack depth is non-dimensionalized against the initial notch root diameter (d = 10.16 mm). Although this curve has been generated for Monel K500, other alloys are easily accommodated by simply scaling the curve by the ratio of elastic modulus (E_{alloy} / E_{Monel_K500}), provided that Poisson's ratio is similar between the two.

We seek to characterize how the overall assembly stiffness changes with crack depth; therefore, we must also define the effective frame stiffness. The effective frame stiffness encompasses the frame, nut, load cell, and all the interfacial contacts that are assumed constant with time. Given the uncertain nature of several of these items, particularly the threaded interface, it is easier and more accurate to empirically quantify the frame stiffness as follows: 1) measure the overall assembly stiffness with an uncracked sample, $k(0)$, 2) retrieve FEA result for uncracked sample stiffness $k_s(0)$, 3) substitute $k(0)$ and $k_s(0)$ into Equation 2 and calculate effective frame stiffness k_f. Once k_f is defined, then the overall assembly stiffness vs. crack depth is readily obtained with Equation 2.

Figure 7 compares the assembly and sample stiffness vs. crack depth, both normalized to their uncracked values. The assembly exhibits lesser sensitivity to crack growth than the sample alone, due to the finite stiffness of the frame components. One clear implication of this result is that the frame must be as rigid as possible to maximize crack growth sensitivity when using a constant-strain load shedding approach.

In practice, Luna's data acquisition software measures the sample force (F) and compares it to the initial preload force (F_0) to obtain the nondimensional assembly stiffness (k/k_0), recalling that the deflection x is constant. Applying the k/k_0 value to the calibration curve developed above provides the corresponding normalized crack depth ($2a/d$). Knowing the uncracked notch diameter, d, the effective crack depth is readily calculated. One limitation of this approach is that there is no provision for assessing eccentric crack propagation in real time, only during post-fracture inspection. However, the highly uniaxial loading afforded by the high-precision sensor geometry tends to promote concentric crack growth, evidenced by the results obtained to date.

EXPERIMENTAL PROCEDURE

In this section, we describe the fracture sample materials tested to date, their preparation for testing, and the general approach used to carry out crack propagation studies in both laboratory and field environments.

Fracture Sample Materials and Preparation

Monel K500 is a prevalent marine alloy for high strength applications including brackets, fasteners and shafts. Despite its low hydrogen diffusivity, K500 component failures due to hydrogen embrittlement have been observed over extended periods within the range of practical cathodic protection potentials[3-5]. This combination of factors made K500 a good candidate material during the development of the EAC sensing platform. Prior to testing K500, however, Luna utilized another marine alloy, 17-4 PH stainless steel, to validate proper operation of the crack sensor mechanics, as this material was more readily embrittled and machined. Table 1 provides heat treatment, strength, and composition information for the specific alloys employed during EAC sensor testing.

Table 1. Fracture sample materials, strengths, and composition.

Name	Condition	UTS / YS	Fe	Ni	Cr	Cu	Nb	Mn	Si	C	Ti	Al	P
17-4 PH (S17400)	H900 (HRc 45)	1450 MPa 1380 MPa	Bal	3.0 5.0	15.0 17.5	3.0 5.0	0.15 0.45	1.0 max	1.0 max	0.07 max	-	-	0.04 max
K500 (N05500)	HF+Aged (HRc 35)	1183 MPa 803 MPa	0.80	Bal	-	28.3	-	0.81	0.04	0.16	0.44	2.88	0.02

Fracture specimens were machined from round bar stock to produce a circumferentially notched geometry with nominal major and minor diameters of 14.3 mm and 10.16 mm, respectively. The notches were machined with a sharp 60-degree tool (R0.025 mm max) using light passes to minimize cold work zone at the notch root that may inhibit crack initiation. The 17-4 PH samples were aged to a high-hardness H900 condition (HRc 45) to further promote crack growth, as these samples were intended for rapid initial screening tests to prove system functionality. Follow on tests with Monel K500 utilized bar stock direct-aged to a hardness of HRc 35. This hardness represents the upper limit of acceptance per NACE standard MR 0175 for seawater environments[6], again selected to promote cracking in this relatively tough alloy. Prior to testing, the sample notch roots were polished with 3 µm diamond slurry and ultrasonically cleaned in isopropanol for 15 minutes.

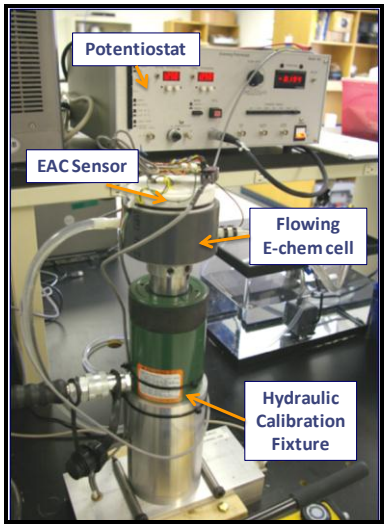

Figure 8. Calibration and RSL test setup.

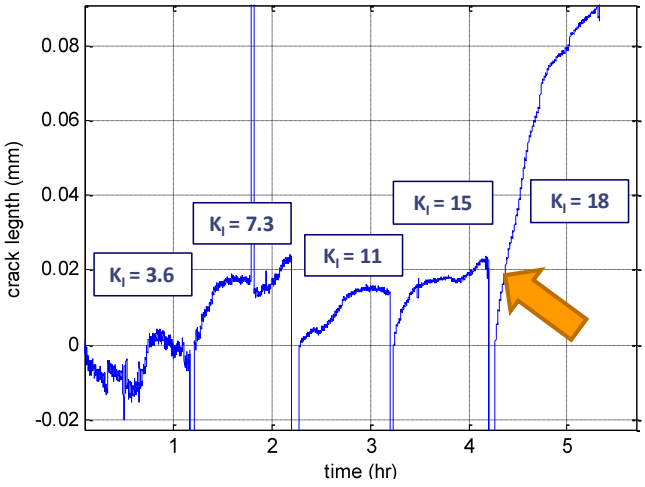

Figure 9. Indicated sample crack depth during RSL test.

Generally, researchers perform crack propagation testing using samples that have been fatigue precracked to improve control of the initiation processes. In this study, starter cracks obtained by rotary

bending fatigue failed to reliably produce concentric starter cracks of the desired depth, resulting in eccentric HE crack growth; an undesirable result as explained in the previous section. The functionality of Luna's EAC sensor permitted a more convenient "precracking" approach wherein a virgin sample is loaded to the desired stress intensity while an aggressive cathodic potential (e.g., -1.25 to -1.4 $V_{Ag/AgCl}$) is applied until the sensor registers crack initiation. When the crack reaches the desired starting depth for the subsequent study, the cathodic over potential is reduced to a protective level (e.g., -0.7 $V_{Ag/AgCl}$) and the sensor stabilized for several hours prior to testing. This method has greatly improved crack depth concentricity and provides a very accurate indicator of starting depth.

Further refinement of the electrochemical precracking method was realized by implementing a rising-step load (RSL) technique, similar to that described in ASTM F1624[7]. By simultaneously applying the cathodic potential and incrementally increasing the load, the minimum stress intensity required for initiating the crack may be found. Lower starting stress intensity enhances the sensor's crack depth measurement range, as the crack may grow deeper prior to ductile overload. Some alloys such as K500 may also benefit from the concurrent application of strain and potential to promote hydrogen uptake. Figure 8 depicts Luna's RSL fixture, with representative results shown in Figure 9 for 17-4 PH at -1.25 $V_{Ag/AgCl}$, where the crack initiates only after the sample stress intensity has increased to 18 ksi-$in^{0.5}$.

EAC Sensor Crack Testing Arrangement

After successful laboratory trials, four EAC sensors were deployed to the Naval Research Laboratory in Key West, Florida for long-term exposure in flowing seawater troughs (Figure 10). Two 17-4 PH SS and two K500 samples were installed, each precracked to 0.1 mm as described above. Figure 11 illustrates the electrochemical connections in the seawater trough: an external Ag/AgCl electrode is suspended proximate to the sensor with an Anomet platinum-coated wire wrapped around the sensor forming the counter electrode. The tensile sample is the working electrode, with electrical connection made through the submersion-rated sensor cable. Polarization of all four sensors was controlled independently by separate manual potentiostats. Crack depth, temperature, and potential data from all sensors was transmitted to a single PC over a digital RS485 bus and stored for further analysis.

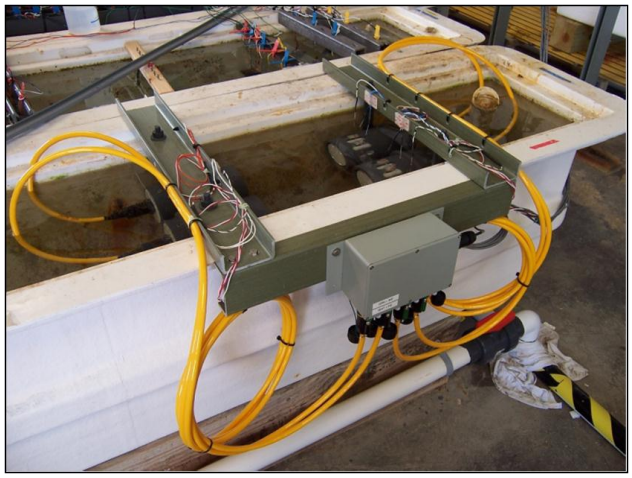

Figure 10. EAC sensor deployment in NRLKW flowing seawater trough.

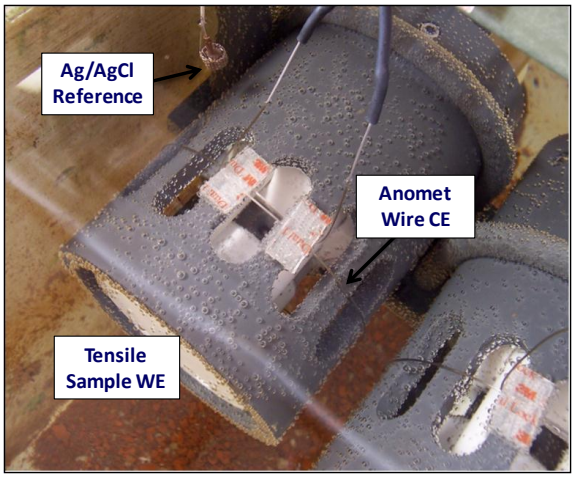

Figure 11. Three electrode arrangement for cathodic polarization of EAC tensile samples.

RESULTS

Initial sensor testing demonstrated the system's ability to observe cracking in the 17-4 PH notched specimens and convert the raw force measurement to a practical depth indication. Figure 12

shows the measured time history for the tensile load for several applied potentials in 0.6 M NaCl solution at an initial stress intensity of 30 ksi-in$^{0.5}$. Translation to crack depth units (Figure 13) reveals the clear trend of crack arrest at open circuit conditions (OCP), reinitiation at -1.05 $V_{Ag/AgCl}$ exhibiting straight-line stage-II kinetics, followed by another arrest period before reinitiating and ultimately entering stage-III fast fracture.

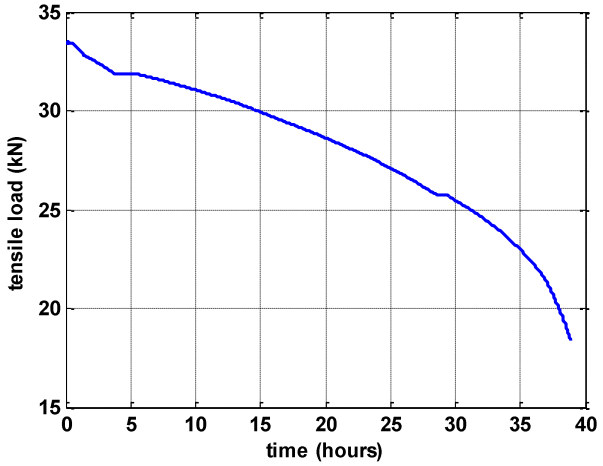

Figure 12. Tensile load time history during 17-4 PH sample crack propagation.

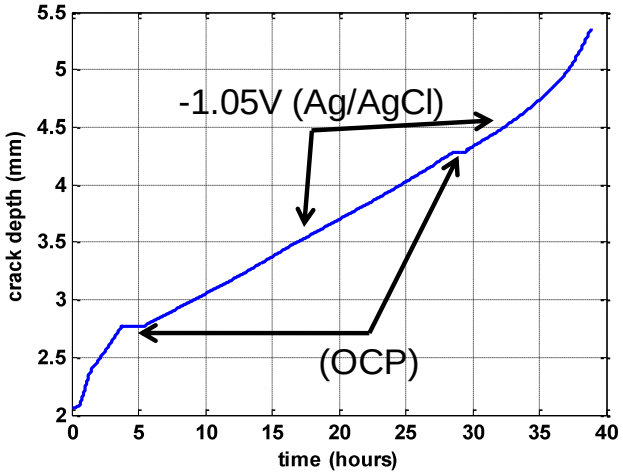

Figure 13. Conversion to crack depth time history, showing periods of stage II cracking and arrest.

A follow-up test was conducted to characterize the sensor output over a range of applied potentials, including less aggressive levels typical of standard anodes. The crack depth time history (Figure 14) demonstrates how the crack velocity readily responds to changes in potential, in this case inflections were noted within seconds of a voltage change. Straight-line fits estimate the crack velocity for each potential, which were obtained using a standard calomel electrode during this particular test. The logarithm of crack velocity is a linear function of applied potential (Figure 15). The logarithmic relationship is physically tractable based on kinetics of the hydrogen evolution reaction given by the Butler-Volmer equation.

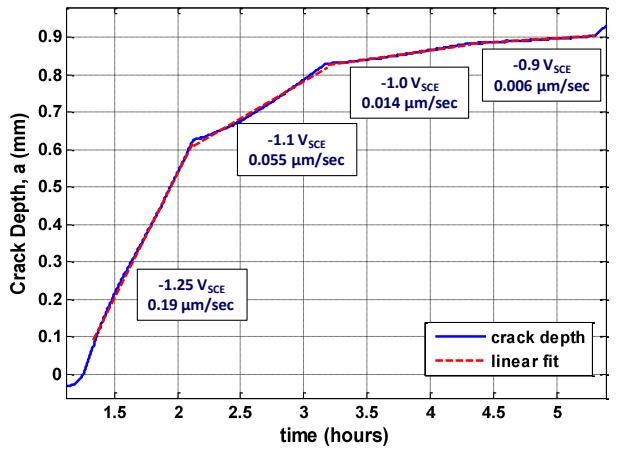

Figure 14. Crack depth time history for 17-4 PH sample over a range of cathodic potentials.

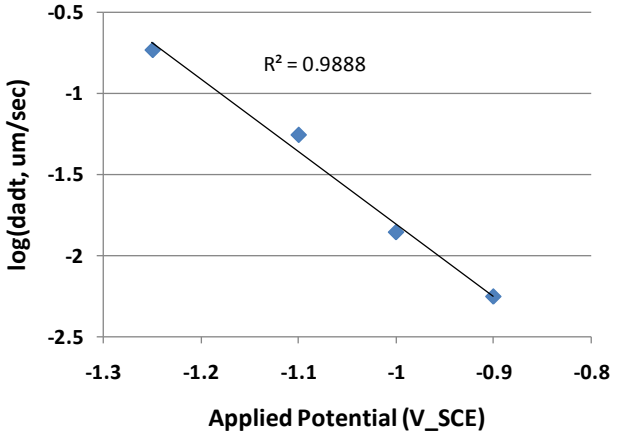

Figure 15. Relationship between measured crack velocity and cathodic potential for 17-4 PH sample.

It is notable that at a very benign potential (-0.9V_{SCE}), the high resolution crack depth transducer was able to quantify a velocity of 0.006 µm/sec in about ten minutes. With this ability to quickly determine crack propagation velocity, minimal sensor life is expended at each potential, allowing multiple conditions to be studied using a single sample that reports velocities in real-time.

After establishing sensor performance with the high-hardness 17-4 PH alloy, Luna's testing transitioned to the higher toughness and slower hydrogen diffusing nickel-based K500 material. After implementing the rising step load approach described above, starter cracks were readily initiated in direct-aged K500 alloy at stress intensities of 25-28 ksi-in$^{0.5}$ in 0.6 M NaCl solution at -1.4 $V_{Ag/AgCl}$. Three K500 samples were precracked to 0.1 mm, resulting in a stress intensity of 30 ksi-in$^{0.5}$. Two of these sensors were deployed to NRL Key West for long-term evaluation at potentials within the range of typical anodes. During the five month test period, the nominal trough water temperature ranged between 18-25 ºC. The remaining sensor was studied at Luna's facility using the same solution as the 17-4 PH samples (0.6 M NaCl, 20 ºC), focusing on more aggressive potentials to permit full sample fracture in approximately one week.

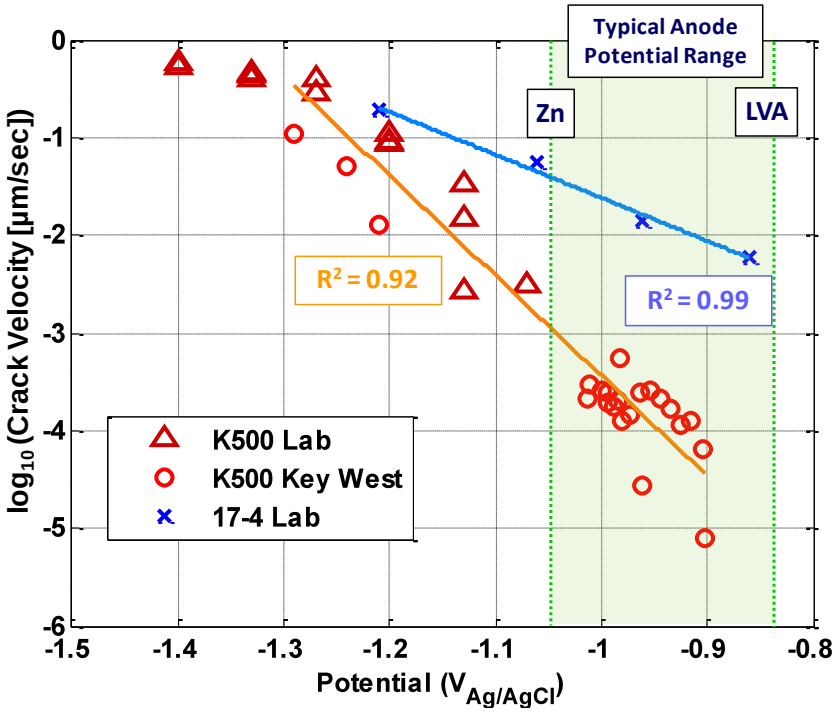

Figure 16. Measured crack velocity vs. cathodic potential for 17-4 PH and K500 samples (K_I = 30-35 ksi-in$^{0.5}$).

Figure 16 presents the results of the K500 studies at both locations, with the log of crack velocity plotted against cathodic potential, including the previous 17-4 PH velocity data for comparison. As with the 17-4 PH material, the K500 sensors exhibit a linear relationship between the log of crack velocity and applied potential over most of the test range, even considering the composite results for all three sensors in two locations (laboratory and Key West). The exception is that at -1.4 $V_{Ag/AgCl}$ the velocity appears lower than suggested by the trend, and this is most likely due to a change in the rate limiting processes for crack growth such as a transition from activation control to diffusion limited kinetics.

Several other interesting observations can be made from this set of data. First, the sensor response reveals non-zero crack propagation (on the order of 0.1 nanometer/sec) within the typical anode potential range, further reinforcing the case for EAC monitoring around critical high strength alloy components attached to cathodically protected structures. Second, while K500 exhibits 100 times slower crack growth than 17-4 PH within the anode range, at -1.2 $V_{Ag/AgCl}$ its velocity nearly reaches that of the high-strength stainless steel, highlighting how quickly damage can occur in K500 if potentials are

not well controlled. In fact, the three Key West data points in the range of -1.2 to -1.3 $V_{Ag/AgCl}$ are associated with an event during which a fault in the potentiostat produced a spike in potential for several hours. Finally, it bears noting again that with four tensile samples (three Monel K500 and one 17-4PH) the EAC sensors were able to generate a large collection of velocity data to characterize the cracking behavior of these two materials, with results available in minutes to days over the wide range of potentials tested.

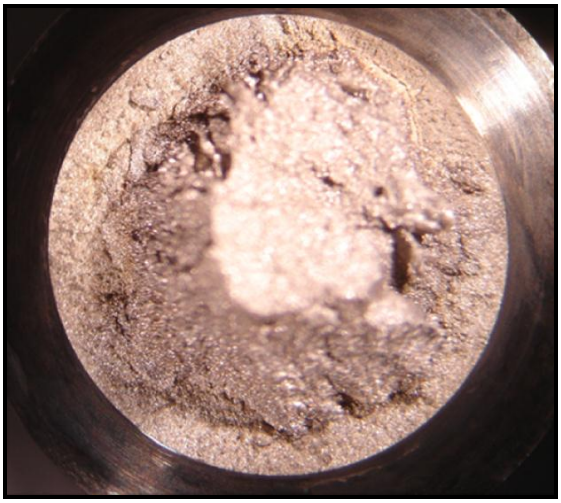

Figure 17: Optical image of K500 fracture surface, showing planar and conical morphology.

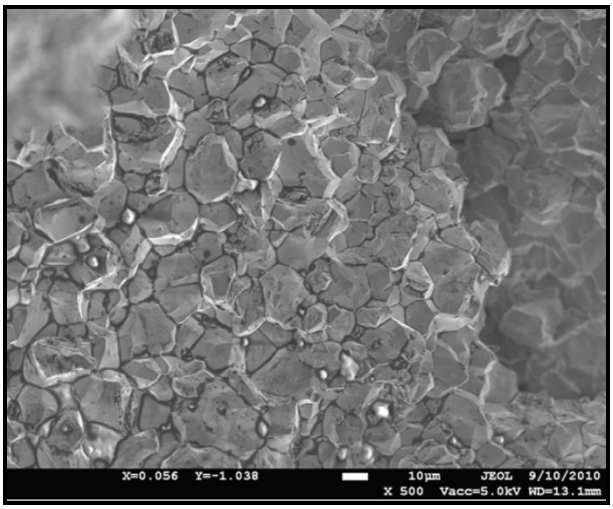

Figure 18: SEM image confirms intergranular cracking across surface (image courtesy of NRL).

As of this writing, the two sensors in Key West have expended only about half of their design lives after six months of crack propagation testing. Luna's accelerated in-house testing produced a fully fractured sample that NRL inspected to ascertain the crack morphology. Figure 17 is an optical image of the fracture surface that appears as a planar concentric crack approximately 1 mm deep, followed by a conical crack surface for the remainder of the 5 mm radial depth. A similar behavior was noted for a previously fractured K500 specimen. Such crack path divergence might be explained by loss of plane strain conditions as the crack propagates through the sample. In any case, the SEM evaluation confirmed that virtually the entire fracture surface exhibited intergranular crack morphology, indicative of hydrogen induced failure.

CONCLUSIONS

- Luna has developed a high-resolution sensing system based on a notched fracture mechanics specimen to monitor environments that might promote cracking, and the susceptibility of alloys to embrittlement. This sensor has been tested in simulated and actual seawater environments to assess cracking behavior in 17-4 PH stainless steel and Monel K500 alloys over a range of applied potentials.

- Very small velocities (~0.1 nm/sec) were observed in direct-aged K500 alloy within the range of typical anodes. With micron-scale crack depth resolution, these low velocities are reliably measurable within a day.

- Crack velocity in both 17-4 PH and Monel K500 were logarithmically dependent on potential; a physically tractable result based on kinetics of the hydrogen evolution reaction given by the Butler-Volmer equation.

- This technology is appropriate for real time alloy characterization in service environments, and structural monitoring to estimate cumulative crack depth.

- Using a single sample, the measurement system is capable of rapid assessment of crack velocity over a range of environmental conditions such as temperature, potential, and solution chemistry.

ACKNOWLEDGEMENTS

The authors would like to thank Dr. Airan Perez (ONR) and Bob Bayles (NRL) for supporting the EAC sensor development technology through an OSD SBIR program (Contract Number N00014-07-C-0731), Brandice Green at NRL Key West for support the sensor deployment and testing, and Lou Raymond for providing important guidance in the use of the RSL techniques.

Any opinions, findings, and conclusions, or recommendations expressed in this material are those of the author(s) and do not necessarily reflect the views of the United States Navy.

REFERENCES

1. R.N. Ibrahim, et al., “Validity of a new fracture mechanics technique for the determination of the threshold steses intensity factor for stress corrosion cracking (KISCC) and crack growth rate of engineering materials”. Engineering Fracture Mechanics, Volume 75 (2008), pp. 1623-1634.
2. H.L. Stark, R.N. Ibrahim, “Estimating Fracture Toughness from Small Specimens,” Engineering Fracture Mechanics, Volume 25, No. 4, pp. 395-401, 1986.
3. R.E. Butler, “Hydrogen Embrittlement of High-Strength Alloys in Marine Environments,” The Institute of Metals 1988, pp. 79-84.
4. J.A. Harris, C.D. Stephens, and R.C. Scarberry, “Effect of Hydrogen on the Engineering Properties of Monel Ni-Cu Alloy K-500,” CORROSION, volume 28, 1972, p. 57
5. J.R. Scully, M.G. Vassilaros, "The Hydrogen Embrittlement Susceptibility of Monel Alloy K-500," Electrochem. Soc. Fall 1983 Meeting, Washington, D.C., October 1983
6. NACE Standard Test Method MR0175-2000, “Sulfide Stress Cracking Resistance Metallic Materials for Oilfield Equipment”.
7. ASTM Standard F1624, 2009, "Standard Test Method for Measurement of Hydrogen Embrittlement Threshold in Steel by the Incremental Step Loading Technique," ASTM International, West Conshohocken, PA, 2003, DOI: 10.1520/F1624-09